Changes in the Organization of the Neuritic Cytoskeleton during Nerve Growth Factor-activated Differentiation of PC12 Cells: A Serial Electron Microscopic Study of the Development and Control of Neurite Shape

J. Roger Jacobs and John K. Stevens

Playfair Neuroscience Unit, University of Toronto, Toronto Western Hospital, Toronto, Canada, M5T 2S8.
Dr. Jacobs's present address is Department of Biological Sciences, Stanford University, Stanford, California 94305.

Abstract. After exposure to nerve growth factor, PC12 cells differentiate within a period of only a few days into cholinergic sympathetic neurons. Using computer-assisted three-dimensional serial electron microscopic reconstruction, we describe the progressive cytoskeletal and structural changes of PC12 neurites at different stages in their differentiation. Developmental changes in these neurites can be characterized by two major transitions. First, microtubules (MTs), which define the longitudinal axis of the neurite, increase in number leading to a more cylindrical and uniform neurite shape. Second, there are major changes in the relative numbers of other organelle types, which reflect the functional specialization of the neurite. These changes do not in themselves seriously affect shape change of the neurite during development, however the presence of these organelles and their associated obligatory volumes (volumes surrounding organelle) account for well over 50% of the neurite's volume at all stages of development. The MT-MT distances and obligatory volumes associated with the organelles remain constant throughout development. Thus, we can conclude that many of the observed changes seen in developing PC12 neurites are due simply to the production of a greater number of MTs in the cell, and that many of the other important parameters that can be measured and contribute to neurite shape remain constant during development.

WHILE the mature axon or dendrite may appear to be a simple physical extension of somal cytoplasm, even a casual examination of its internal structure reveals many differences. The axon, for example, has excluded many organelles that characterize somal cytoplasm, including the Golgi apparatus, rough endoplasmic reticulum, and centrioles (Peters et al., 1976). Moreover, many of the subcellular elements that are shared by the soma and neurite, such as the microtubules (MT),[1] intermediate filaments (IFs), agranular reticulum (AR), and mitochondria have dramatically different cytoplasmic organizations. The mature axon has a highly structured and ordered "cytoskeleton" while little or no order seems apparent within the somal cytoplasm (Yamada et al, 1971; Lasek, 1982; Lasek and Hoffman, 1976; Stearns, 1981).

In contrast, the immature axon seems to have more structural similarities with somal cytoplasm than it has to a mature axonal cytoplasm. Developing axons contain a large number of membranous organelles (Luckenbill-Edds et al., 1979) with few MTs and neurofilaments (Tennyson, 1970; Hoffman et al., 1984), appear to have little organized structure, have very irregular external shapes, and are capable of a greater variety of morphogenetic behaviors when compared with mature axons. Our focus in this paper is on the developmental process that begins with the unstructured somal-like cytoplasm of the young neurite and ends with a highly ordered, adult neuritic cytoskeleton.

An attractive model system for neurite development has been the pheochromocytoma tissue culture line known as PC12. PC12 cells are tumor cells derived from adrenal chromaffin cells of the rat (Greene and Tischler, 1976, 1982). They develop from the neural crest, and do not lose the potential to develop neurites. After exposure to nerve growth factor (NGF), PC12 cells (like normal chromaffin cells) differentiate within a period of only a few days into cholinergic sympathetic neurons with what appear to be normal axons (Unsicker and Chamley, 1977; Dichter et al., 1977). Finally, using time-lapse photography we have verified that PC12 neurite development is indistinguishable from that described for normal nerve cells (Jacobs, 1985; and Jacobs, J. R., and J. K. Stevens, manuscript in preparation). A number of authors have described morphological changes in PC12 cells that occur after NGF activation (Connolly et al., 1979; Luckenbill-Edds et al., 1979; Greene and Tischler, 1976, 1982; Hickey et al., 1983). In this report, using

1. *Abbreviations used in this paper*: AR, agranular reticulum; MAP, microtubule-associated protein; MT, microtubule; IF, intermediate filament; NGF, nerve growth factor.

computer-assisted three-dimensional serial electron microscopic reconstruction we extend these observations and describe the progressive cytoskeletal and structural changes of PC12 neurites at different stages in their differentiation. In the following report, we will describe experimental manipulations of PC12 neurites during development.

Materials and Methods

Cell Culture

PC12 cells (provided by L. A. Greene, Department of Pharmacology, New York University Medical Center) were maintained in Dulbecco's modified Eagle's medium (Gibco, Grand Island, NY) containing 5% fetal calf serum, 10% heat-inactivated horse serum (KC Biological Inc., Lenexa, KS), 2 mM L-glutamine, 1% non-essential amino acid, and 20 μg/ml gentamycin. Cells were propagated through a maximum of 20 passages before renewal from original stock. It was found that continuation of a PC12 line beyond this time permitted cells that demonstrate no gross morphological response to NGF to dominate the culture. However, the timetable of NGF response in those cells which retain their sensitivity does not alter through successive generations.

Cells were grown on collagen-coated dishes. Morphological differentiation was induced by replacing growth medium with Dulbecco's modified Eagle's medium supplemented with 1% heat-inactivated horse serum and 100 ng/ml NGF (generous gift of J. Reid, University of Toronto). Cultures were fed every 3 d. Tissue culture protocol was similar to that described by Black and Greene (1982).

Fixation

Results reported here come from PC12 cultures fixed after 3, 6, 8, 18, 22, or 43 d in NGF. Cultures were fixed for 1 h at room temperature in 0.1 M sodium cacodylate (pH 7.30) with 2% glutaraldehyde (Eastman Kodak Co., Rochester, NY). Postfixation with 1% osmium tetroxide and 1% potassium ferrocyanide in sodium cacodylate buffer was for 90 min. Cultures were then dehydrated through 50, 70, 90, 95, and 100% ethanols before infiltration and embedding in Epon 812 (Ted Pella, Inc., Irvine, CA). Twelve other fixation protocols were also tried varying both in ingredients and concentrations. This fixation was chosen over the other protocols because it provided reliable preservation of ultrastructure and good contrast to the widest variety of ultrastructural features, while still preserving microtubular integrity. Potassium ferrocyanide enhances contrast of lipid- and glycoprotein-containing structures (Bullock, 1984; Goldfischer et al., 1981) and in our experience, reveals regional differences in the cytoplasmic "ground substance" that proved useful in the analysis of MT organization in neurites.

Sectioning and Electron Microscopy

The techniques used for thin sectioning and staining long series of Epon-embedded material have been described elsewhere in detail (Stevens et al., 1980; Stevens and Trogadis, 1984). Briefly, a ribbon of consecutive sections, detached from the diamond knife with a fine hair, is collected with a fine wire loop, and deposited upon a formvar-coated (0.5% solution) rigid copper-berillium slot grid (Synaptek; Ted Pella, Inc.). After staining in 8% aqueous uranyl acetate followed by 0.025-M lead citrate in 0.01 N NaOH, grids were placed in protective copper cassettes and photographed by a JEOL 100CX electron microscope on 3¼- × 4-inch negatives. Data reported here were obtained from material photographed at magnifications of 13,000 or 18,000.

Computer-assisted Reconstruction

All quantitative analysis of electron micrographs used a computer-assisted serial reconstruction system previously described (Stevens et al., 1980; Stevens and Trogadis, 1984).

Experimental Design

Complete three-dimensional reconstructions for quantitative analysis were taken from fixations after 3, 8, and 43 d in NGF. This choice is based upon the analysis of time-lapse data (Jacobs, 1985; Jacobs, J. R., and J. K. Stevens, manuscript in preparation) demonstrating that PC12 neurites exhibit a wide variety of very active, morphogenetic changes in the first week after NGF activation. From the sixth to the eighth day in NGF these behaviors rapidly decline, and the first long-lived neurites begin to appear. 3-d neurites were reconstructed to provide information on the structure of young, "labile" neurites. 8-d neurites are transitional, and 43-d neurites represent the final "mature" neurite morphology. That is, the length and shape remain relatively stable and prominent growth cones seem to be absent from the neurite's tips.

All statistics are based upon normal parametric analysis unless otherwise specified.

Microtubule Analysis

Calculation of MT lengths (L) from $L = 2Na/T$ is based upon the estimation used by Hardam and Gunning (1978) and Chalfie and Thompson (1979) where N, a, and T are average number of MTs per section, the length of the series (in micrometers), and the number of terminations in the series, respectively.

Histograms of distances between MTs were created in the following manner. Using the computer reconstruction system, points were placed in the center of all MTs within a given cross section. The distances between each point to each adjacent point were computed. The minimum distance for a given point to an adjacent point was taken as the minimum intermicrotubule (inter-MT) distance. These distances were compiled for many sections to create a histogram similar to that shown in Fig. 8. To test the equivalence of the means of the distribution of inter-MT distances, the approximate t test for means of unequal variance (two-tailed) was used (Sokal and Rohlf, 1969).

Organelle Volume Analysis

Estimates of volume contributions made by individual and groups of organelles were made using a method described in Sasaki et al. (1984). The volumes of individual sections from reconstructed neurite were plotted as a function of length or section number assuming a section thickness of 0.1 μm (see Figs. 5 and 6). This will be referred to as the neurite volume. The sum or integral of these components would approximate the total volume of the neurite. On the same graph we plotted the organelle volume section by section and the "effective volume" of the MTs. The effective volume of MTs was computed making certain assumptions using the inter-MT histogram discussed above as well as other assumptions that will be described in Results, and discussed in detail in the following paper. Regions where the neurite volume expanded into a varicose region were picked using criteria similar to those outlined in Sasaki et al. (1984). The total volume of these regions and the total volumes of the organelles contained in these regions were computed to produce the plot shown in Fig. 9. In this analysis, a total of 17 regions were analyzed.

Linear regressions are based upon "Model one" assumptions. These assumptions are as follows: (*a*) the independent variable is measured without error; (*b*) the dependent variable varies linearly with respect to the independent variable; (*c*) values are normally distributed; and (*d*) variance is independent of the magnitude of the variable. There were not enough data to fully test all these assumptions. Confidence limits for slopes and testing of hypotheses for equivalence of slopes are based on the t test statistic (Sokal and Rohlf, 1969). Volume data on all membranous organelle types were treated identically, based upon the results of Sasaki et al. (1984) which established the equivalence of all membranous organelle types in volume contribution to neurites.

Results

Overview of PC12 Neurite Development

Previous work based on time-lapse observations of PC12 cells (Jacobs, 1985; Jacobs, J. R., and J. K. Stevens, manuscript in preparation) suggested three basic phases of neurite development. The soma starts as a small, almost spherical cell <10 μm in diameter (Fig. 1). Soon after NGF activation, the soma becomes larger and small spike-like neurite buds (pseudopodia and filopodia) appear over the entire cell surface. The most prominent buds develop at the base of the soma to adhere to the surface of the dish (2-d cell; Fig. 1). These young neurites have a highly irregular shape, when compared with the more mature processes (see Fig. 4). For

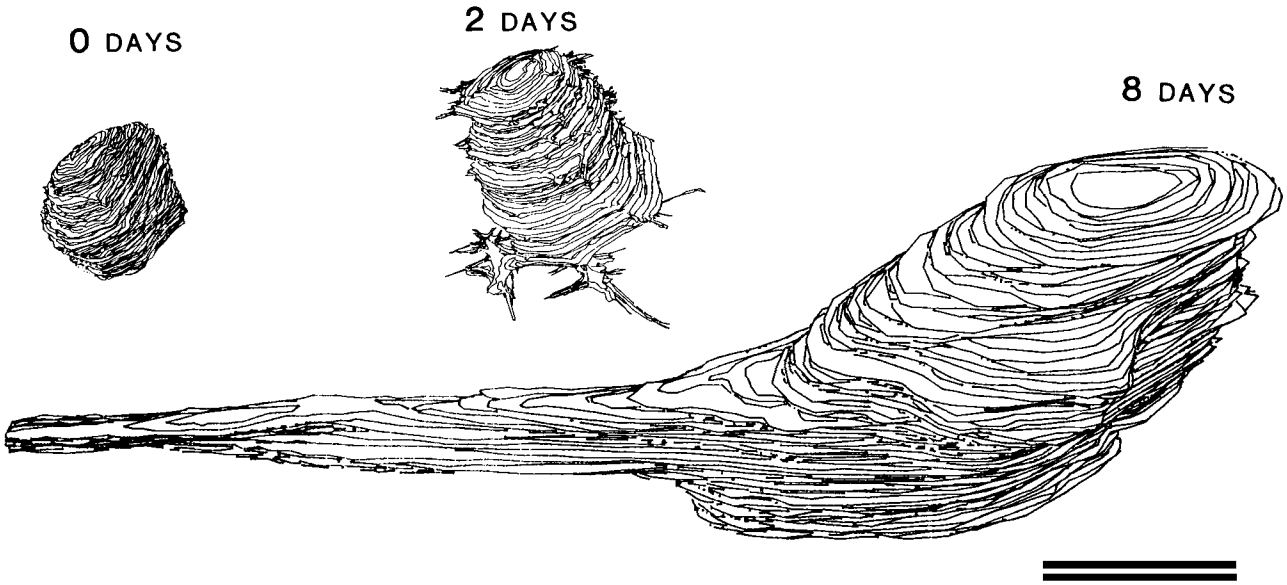

Figure 1. Complete PC12 soma reconstructions during differentiation. Three typical reconstructions of a PC12 soma before NGF induction, shortly after induction, and during development of final neuronal form are shown together here at the same scale. Note the increase in somal size and the development of a large neurite during differentiation.

the next 4–7 d, the cells display highly labile and mobile behavior. This first phase is followed by a transitional period in which the neurite becomes more structurally stable with a more regular axial shape. Finally, after 8–12 d, the soma has expanded to many times its original volume and the neurite develops a full stable morphology with an approximately cylindrical axial cross section (see 8-d cell; Fig. 1).

In this study a total, of 27 three-dimensional electron microscopic reconstructions were carried out from 12 sets of serial sections cut from eight different fixations, each focused on one of these three stages described above. This represents reconstruction of over 1,000 total micrometers of microtubules, and over 5,000 total serial sections. We report details on only 13 complete reconstructions of neurite seg-

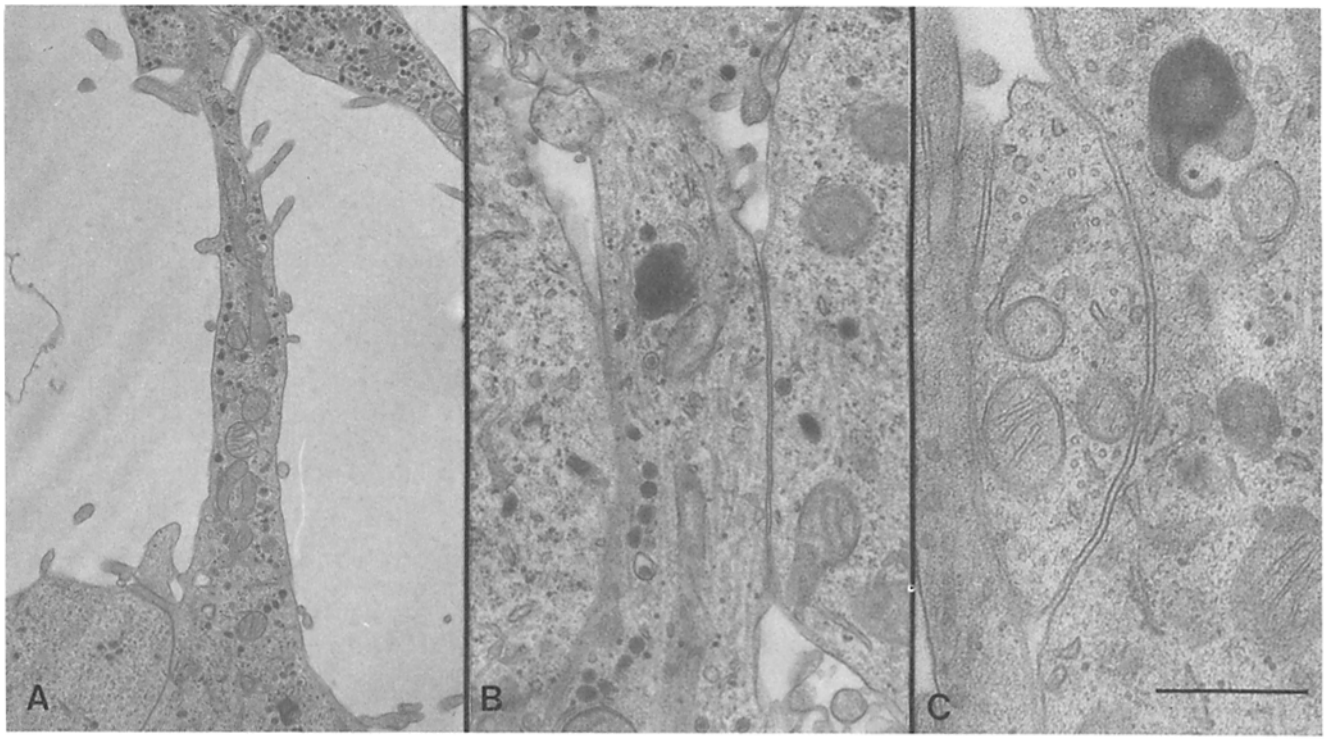

Figure 2. Ultrastructure of young PC12 neurites. *A* and *B* are longitudinal sections and *C* is a cross section from "young" neurites extended by PC12 cells within 3 d of NGF addition. Note the irregular external contour, low density of MTs, and the large number of membranous organelles. Bar, (*A*) 2 μm; (*B* and *C*) 0.4 μm.

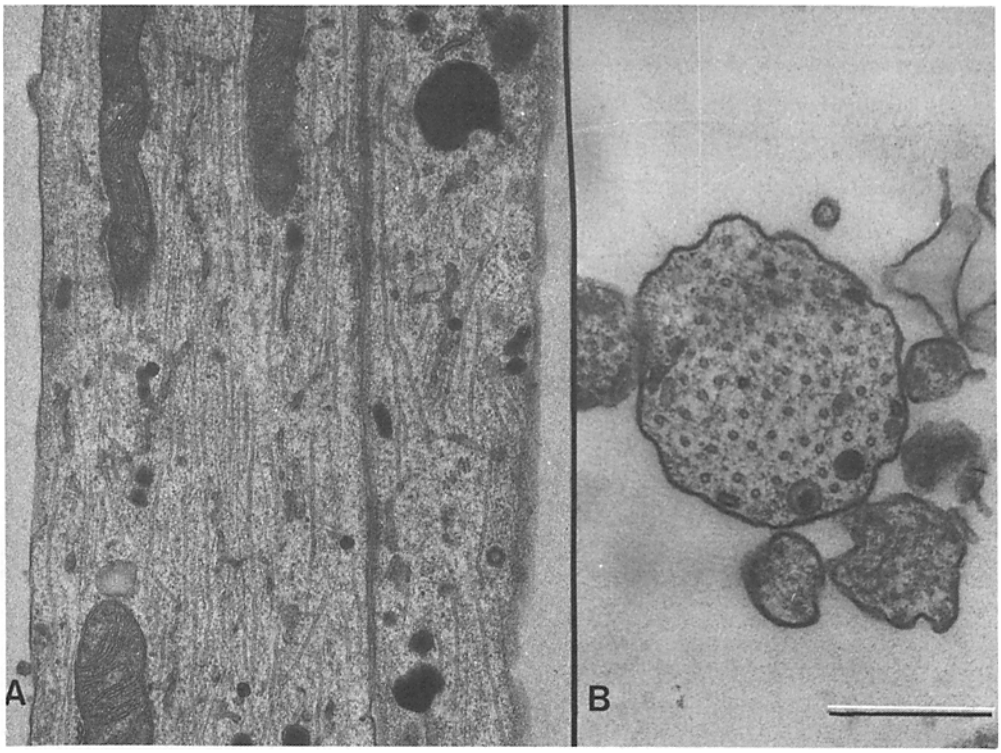

Figure 3. Ultrastructure of mature PC12 neurites. *A* is a longitudinal section and *B* is a cross section through a "mature" neurite of PC12 cells after 43 d in NGF. In contrast to Fig. 2, neurites are circular in cross section, have many more MTs, and organelles show a longitudinal orientation in the neurite. Bar, 0.4 μm.

ments, all of which include MTs, organelles, and the outer plasmalemma. Specifically, this group includes four complete neurites 3 d after NGF activation as representative of the labile phase, five neurites 8 d after NGF as transitional neurites, and four neurites at 43 d as examples of mature neurites. All complete PC12 neurite reconstructions upon which the following quantitative analysis is based are illustrated in Fig. 4.

A simple survey of single section electron micrographs of PC12 neurites is shown in Figs. 2 and 3. Young PC12 neurites (Fig. 2) differ from mature neurites (Fig. 3) in several important ways. First, the young neurites have an irregular external contour which presumably permits maximum contact with adjacent structures. In contrast, the external contour of mature neurites tend to be circular in cross section. This difference is also demonstrated in the cross sections drawn in Fig. 4. Secondly, young neurites contain a large number of irregularly shaped membranous organelles (mitochondria, AR, chromaffin granules, multilamellar bodies, multivesicular bodies, and large dense granules). In comparison, mature neurites have many more MTs, and membranous organelles are longitudinally oriented within the neurite.

Analysis of complete three-dimensional reconstructions of neurites reveals quantitative relationships between many ultrastructural features and these are considered below.

Microtubule Organization in PC12 Neurites

Reconstructions of microtubular arrays in both mature (43 d in NGF) and immature neurites (3 d) are shown in Figs. 5 and 6. The MTs at all three stages seem to be arranged in "woven" non-parallel tracks. Similar observations were made in our previous study on dendrites (Sasaki et al., 1983). However, in contrast to dendrites, it was not at all uncommon to find many MTs come into close association to form a parallel sheet around groups of organelles.

It is also clear from these analyses that on average the immature neurites have fewer MTs when compared with the intermediate and adult neurites. These differences have been quantified and will be presented in more detail below.

Microtubule Terminations and Length

Analysis of serially reconstructed MTs are summarized in Table I. Only MTs from complete neurite reconstructions are included in this analysis. The table shows that calculated MT length (see Materials and Methods) increased with increasing time after NGF addition. It also shows that three-quarters of all MT terminations were in the close vicinity (i.e., within 70 nm) of membranous organelles or plasma membrane. In contrast to our previous work on retinal dendrites (Sasaki et al., 1983), there was not a significant polarity of terminations (e.g., plasmalemmal endings found, but no beginnings) within any series.

MT–MT Minimal Distances and MT Exclusion Zones

It is well documented in other systems that MTs in neurites seem to organize themselves in regular arrays with a minimal distance between adjacent MTs and structures. Figs. 3 and 7 show that the PC12 MT array is also very uniform and MTs appear to maintain a preferred distance with neighboring MTs. We have quantified these MT–MT distances using methods similar to those used in our previous work (Sasaki et al., 1983).

Distances between MTs and their nearest neighbor MT were calculated for neurites from PC12 cultures fixed after 3, 8, and 43 d in NGF using a histogram method that has been previously described (see Materials and Methods). The distribution of inter-MT distances summarized in the histograms shown in Fig. 8 demonstrates three consistent features. (*a*) An absolute minimum inter-MT distance of 36 nm is never violated. This is 12 nm in addition to the average 24-

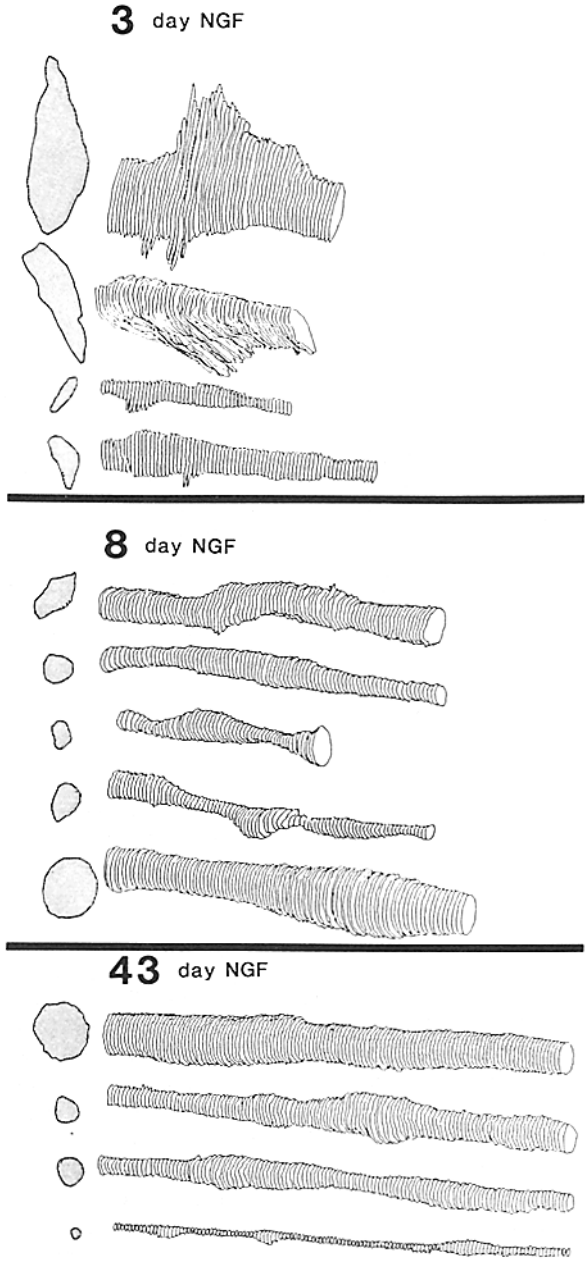

Figure 4. Profiles of reconstructed neurites. The outer plasmalemmal contour of the totally reconstructed neurites used in the quantitative analysis are shown here to the same scale. At left is a representative cross-sectional profile from the same neurite. The horizontal lines represent 10 μm.

Table I. Summary of Microtubule Reconstructions

Microtubule lengths			Microtubule terminations		
Days in NGF	Total microtubule length reconstructed	Calculated microtubule length	Days in NGF	Per μm microtubule length	Location (ORG/PM/?)
3	134.2	17.7	3	0.17	16/6/1
8	98.2	22.3	8	0.18	4/5/0
43	310.7	58.8	43	0.05	16/4/3

First three columns summarize total microtubule length reconstructed and the microtubule length, calculated as described in Materials and Methods, for each experimental age. The latter three columns summarize all data on microtubule terminations. All terminations were classified to be on membranous organelles (*ORG*), the plasmalemma (*PM*), or not near any identifiable structure (*?*). All units are given in micrometers.

nm MT diameter. (*b*) The average MT-MT distance (69 nm) does not shift significantly during development. (*c*) In very young neurites (after 3 d in NGF), which have fewer MTs and smaller MT arrays, the scatter of inter-MT distances is very broad (SD = 30 nm).

For the transitional (8 d in NGF) and mature (43 d in NGF) neurites, which have more MTs, MT arrays become more regular, and the standard deviation of inter-MT distances declines (SD = 15 nm).

Conceptually the regular spacing pattern between MTs in neurites creates a volume component beyond the actual MT, smaller but similar to that described by Sasaki et al. (1983) in dendrites. On occasion, staining made it possible to actually see this additional volume as shown in Fig. 7 *E*. The ferrocyanide staining process occasionally exposes electron-lucent zones surrounding each MT similar to that described by others (Porter, 1966; Behnke, 1975; Schliwa, 1978). These zones average 65 nm in diameter (SD = 6 nm, $n = 41$). Other organelles, including other MTs, do not invade this zone. This value is very close to the mode of the MT-MT histogram shown in Fig. 8 of 69 nm.

These zones were often demarcated because they exclude sheets of membrane (or "membranous veils") that are extruded from cisternae of AR (see Fig. 7 *E*). Membranous veils have only been seen in ferrocyanide-stained material, which is known to enhance contrast of lipid-containing structures. Continuity of membranous veils with AR is demonstrated in the series of sections shown in Fig. 7. MT exclusion zone fenestrations through these sheets are seen in both mature neurites (Fig. 7 *E*) and young neurites.

Intermediate Filaments

IFs (10-nm IFs or vimentin) are not a dominant feature in PC12 neurites. IFs were seen very rarely in young neurites. In mature neurites, clusters of six or more neurofilaments are occasionally seen. If a large number of inter-IF distances are measured, a mean of 26 nm is found or 16 nm in addition to IF diameter.

Obligatory Organelle Volume

It was clear from our earlier work (Sasaki et al., 1984) that organelles contained within neurites have an obligatory volume that goes beyond their own volume and that this volume has the potential to play an important role in the development and control of PC12 neurite shape. We have, therefore, repeated an analysis similar to that described in Sasaki et al. (1984, see also Materials and Methods) on these PC12 neurites at various stages in their development.

Examples of plots used to determine the obligatory volume constant are shown in Figs. 5 and 6, and a plot of all compiled data is shown in Fig. 9. In Figs. 5 and 6, the total volume of each section is plotted as a function of the section number (upper curve). Below that curve is a plot of the total organelle volume, the effective volume of the MTs, and the AR volume. On the top of each figure is the actual reconstruction. This makes a quantitative comparison possible of intracellular components with the volume and shape of the plasma membrane.

The graph in Fig. 9 shows the total varicosity volume vs. the total organelle volume compiled for all ages of cultures. 3-d neurites are shown as squares, the 8-d neurites as stars and the 43-d neurites as circles. In each case, neurite volume

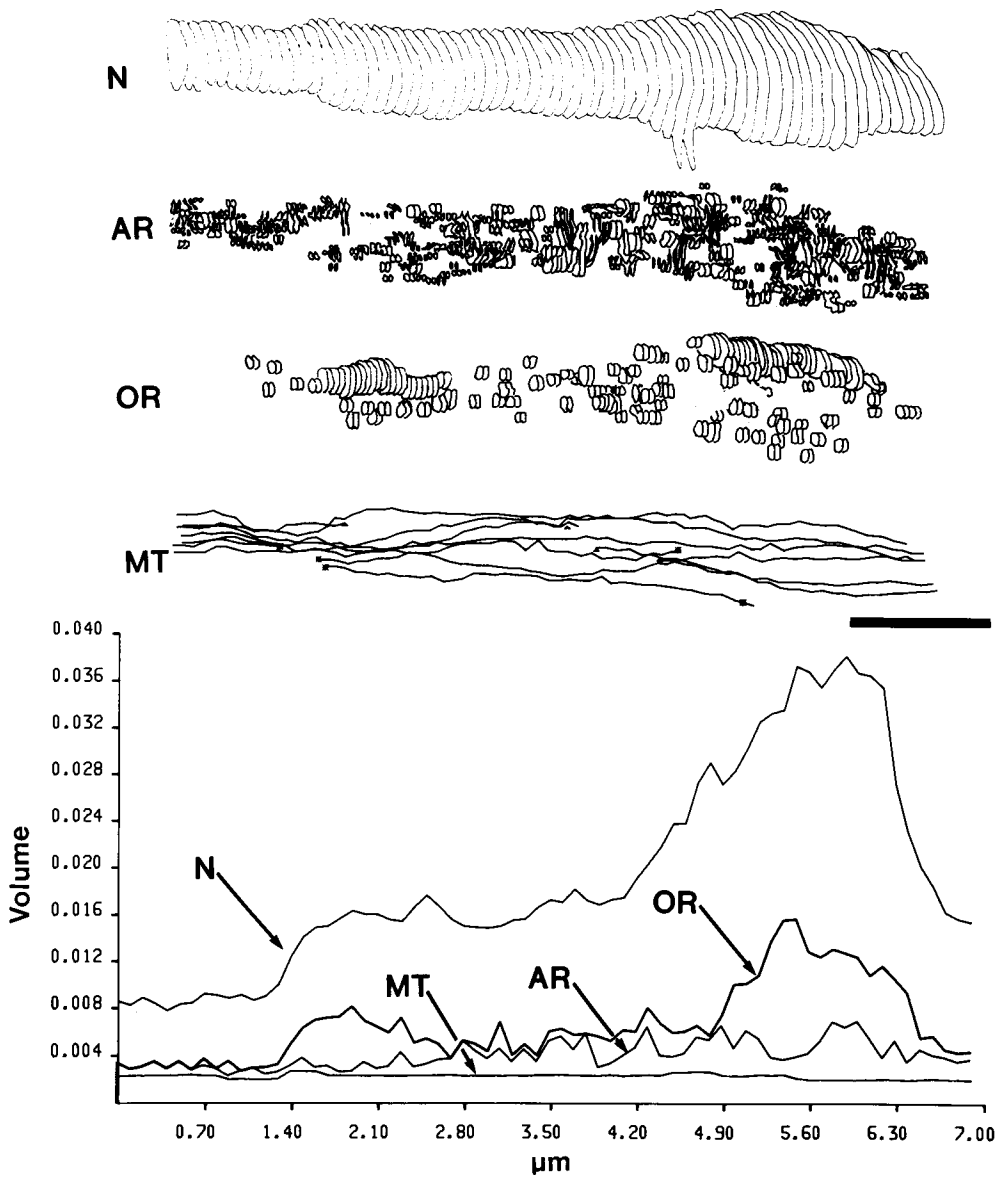

Figure 5. Volume analysis of a young PC12 neurite. The upper half of the figure presents computer-generated plots of each component of a complete reconstruction of a neurite after 3 d in NGF. On top is the outer neurite plasmalemmal contour (*N*), the agranular reticulum (*AR*), other membranous organelles (*OR*), and the completely reconstructed microtubules (*MT*). MT endings are marked with a small asterisk. The lower half of the figure presents a section-by-section analysis of the volume contribution of each neurite component as plotted above. The ordinate is the total volume of reconstructed organelles, and the abscissa is length along the neurite. The graph of each component is added to the previous, beginning with MTs, then AR, and finally total membranous organelles. Note the clustering of organelle volume coincides with the location of the much larger neurite varicosity. MT volume and AR volume are more uniformly distributed. Bar, 1.0 μm.

data were corrected for MT volume. Each micrometer of MT was attributed 0.0054 cubic micrometers of volume, which is 1.42 times the volume of a 1-μm length of MT exclusion cylinder (assumed diameter = 69 nm). The rationale for this approach is presented in the following article. A regression analysis was performed with this data and the membranous organelle volume for each corresponding neurite region; it shows a very tight correlation between the local neurite volume and the local organelle volume that seem not to change for different age cultures. Neurite volume (*Vn*) is 4.52 times organelle volume (*Vo*) ($r = 0.998$, $n = 17$, 90% confidence limits are 4.52 ± 0.37). Thus, the obligatory volume constant appears to be a stable 4.52 throughout development.

Changes in Neurite Composition during Neurite Maturation

Comparisons of these reconstructions of neurites reveal that organelles are not distributed uniformly in PC12 neurites and even casual examination of the micrographs in Figs. 3 and 4 shows that changes in number and distribution of organelles occur after NGF activation. Generally, the smooth endoplasmic reticulum or the agranular reticulum (AR) is uniformly distributed throughout the volume of the neurite. Chromaffin granules retain a uniform distribution as well, and are found in close association with the AR. Dense bodies, multilamellar bodies, multivesicular bodies, and mitochondria tend to cluster in regions where neurite caliber is increased. These regions will be referred to as varicosities. There is little regional variation in MT number along neurite length. Relative volumes of each kind of organelle reconstructed in neurites and relative contributions of each group are compared for each age in Fig. 10. Again as discussed above, MT volume was assumed to be the volume of a cylinder around each MT of 69 nm in diameter. This value was obtained from the inter-MT distance (Figs. 8 and 9). It is clear that total MT contribution to volume rises continuously during neurite ontogeny from 8% total volume to >25%. IF volume was calculated in a similar way, from the mean inter-

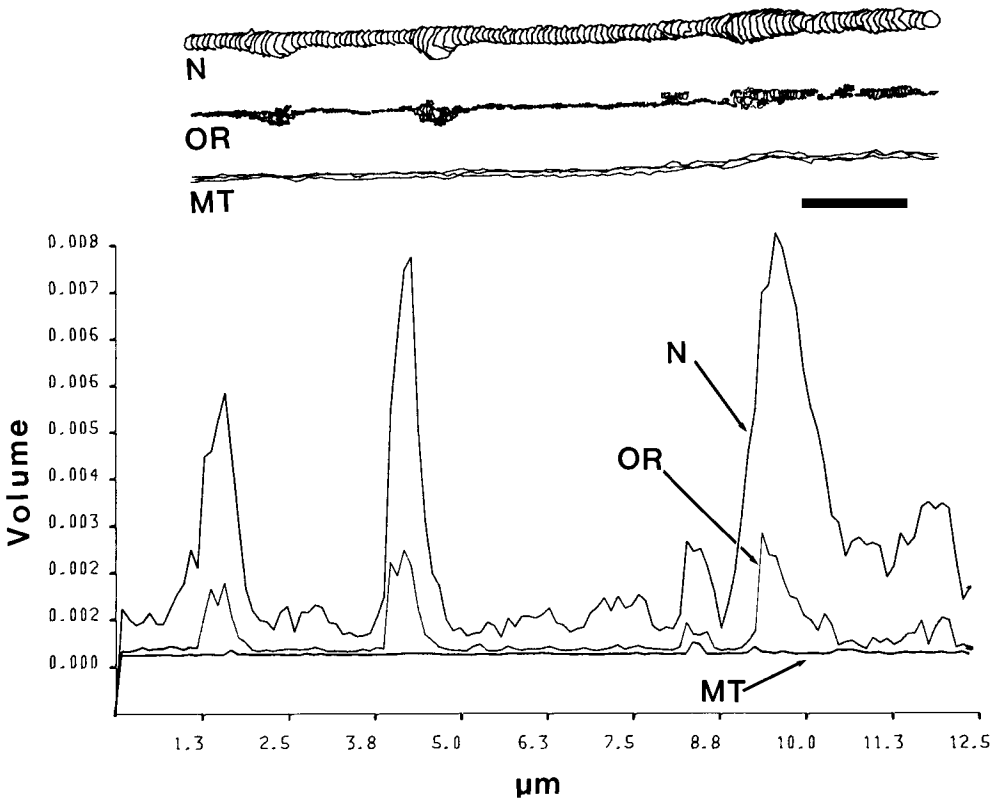

Figure 6. Volume analysis of a mature PC12 neurite. A volume analysis of a neurite reconstruction after 43 d in NGF is shown according to the same format as in Fig. 5. This is an unusual mature neurite in that it contains only three continuous MTs. Note, however, that it is consistent with the observation that total volume occupied by the MTs relative to other components increases over time. We use it however here because it clearly demonstrates how varicose neurite expansions coincide with clusters of organelles. Bar, 1.0 μm.

IF distance of 26 nm. IFs, though not present in young neurites, account for ~1% of total volume in mature neurites. Mitochondria are prominent in young neurites (8%), declining dramatically in mature neurites (<1%). The same is true for chromaffin granules (4.4% drops to 1.6%). In contrast, dense body organelles (which includes multilamellar bodies and multivesicular bodies) increases in volume with maturation (from 1.6 to 4%). The AR remains very constant through all stages of maturation in PC12 neurites.

Discussion

The Ontogeny of Neurite Ultrastructure

This paper describes the quantitative and qualitative changes in PC12 neurite composition during differentiation. A young neurite contains few MTs, no neurofilaments, and a wide variety of membranous organelles. Neurite shape is irregular and its internal structure is not highly organized. In contrast, a mature PC12 neurite is dominated by MTs, has some IFs, and contains fewer membranous organelles. Neurite shape is more cylindrical and internal structure is very ordered. The average MT length increases after NGF activation, but the MT–MT minimal distance or MT exclusion zone remains constant, and the obligatory volume associated with organelles remains constant. Thus, one could conclude that the observed changes in PC12 neurite shape and its development are due primarily to changes in quantity and number of intracellular elements – not qualitative changes in the intracellular elements themselves. The contribution of each organelle type to neurite composition is discussed below.

Microtubules

The MTs are a dominant feature of the mature axon. We have corroborated previous reports (Peters et al., 1976) that the density of MTs rises during neurite differentiation. In young neurites, when MT density is still low, membranous organelles can maintain random orientations with respect to the axis of the neurite. In addition, the neurite contour in cross section is very irregular, presumably changing shape to conform to the surroundings. In mature neurites, an increased MT density correlates with increased neuritic organization. Neurite profiles are round, in spite of external influences, and membranous organelles are longitudinally oriented within the neurite.

Microtubule Exclusion Cylinders

Each MT exists at the center of its own cylinder of influence, described earlier as the MT exclusion cylinder. The perimeter of this cylinder tends to associate with the perimeter of other MT exclusion cylinders, as well as with the inner surface of the plasmalemma or membranous organelles. The MT exclusion cylinder has also been described in neuronal dendrites (Sasaki et al., 1983), plant root hair cells (Porter, 1966), red blood cells (Behnke, 1975), and angelfish melanophores (Schliwa, 1978). This cylinder is normally electron lucent (Behnke, 1975; Schliwa, 1978; this study) but a filamentous component can be stained with some heavy metals in nervous tissue (Burton and Fernandez, 1973; Smith et al., 1977).

It has been proposed that microtubule-associated proteins (MAPs) which coat the surfaces of MTs account for the volume of the MT exclusion cylinder (Dentler et al., 1975;

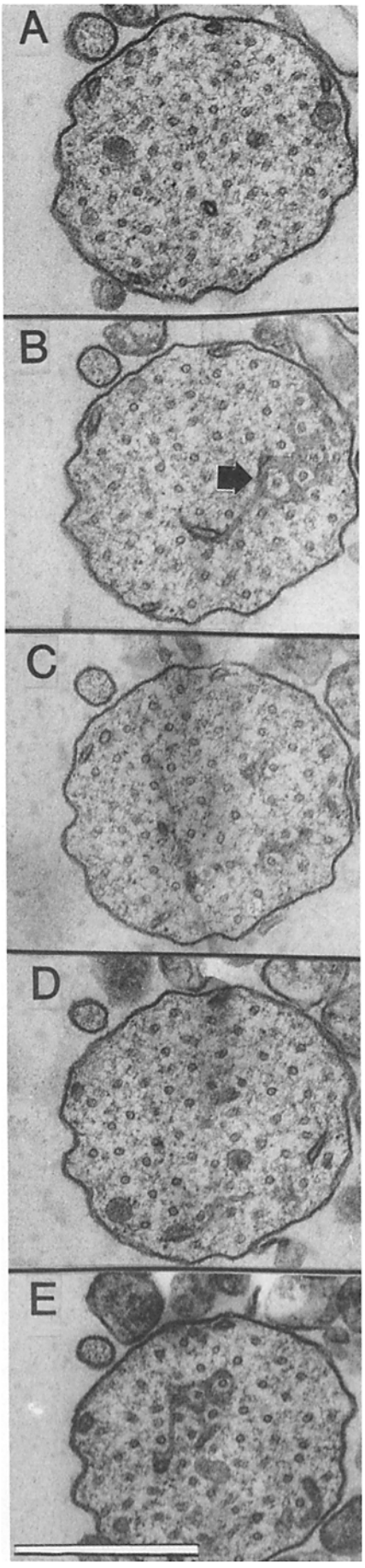

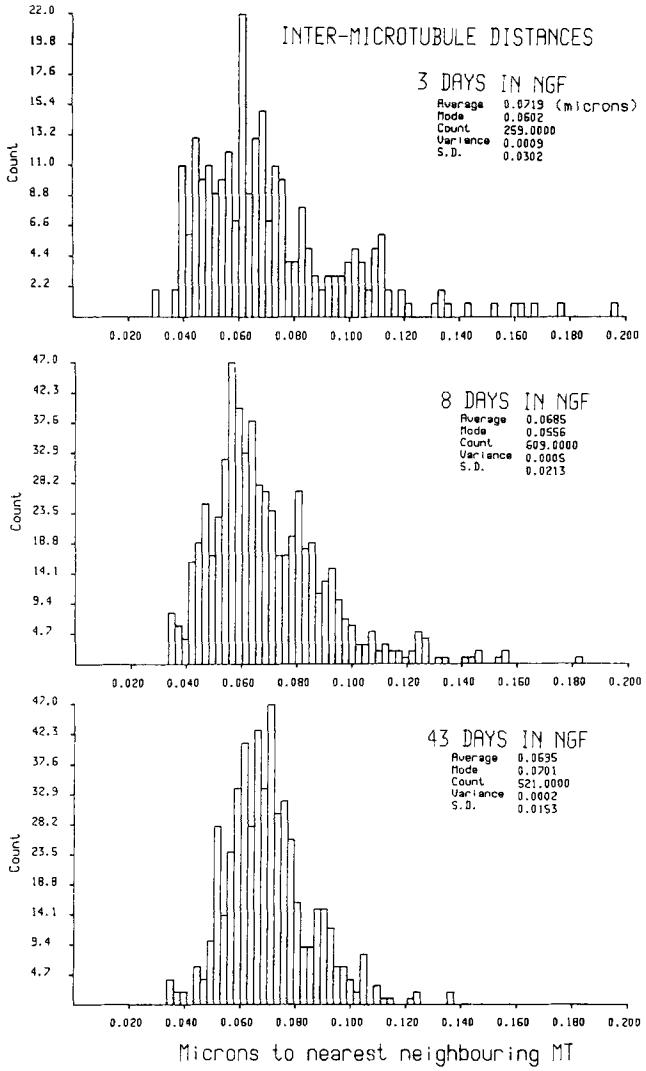

Figure 8. Distribution of intermicrotubular distances. The distance between any MT and its nearest neighbor (abscissa) is recorded from a large, randomly sampled population of MTs in cross section. The distribution of these distances is plotted for neurites after 3, 8, and 43 d of exposure to NGF.

Langford 1983; Sasaki et al., 1983). Different values have been reported for the diameter of the MT exclusion cylinder. In this study, the cylinder diameter is 69 nm, similar to 60–70 nm for angelfish melanophores (Schliwa, 1978) and 66 nm in insect ovary (Stebbings and Bennett, 1975) but less than preferred inter-MT distances of 75 nm in dorsal root ganglion cells in culture (Yamada et al., 1971) and 94 nm in cat retinal ganglion cell dendrites (Sasaki et al., 1983). These differing lengths are consistent with the fact that MAPs of differing molecular weights (and likely differing size) are found in different cell types, and even different regions of the same cell (Matus et al., 1983; Bloom and Vallee, 1983; Wiche et al., 1983). Most importantly, these data suggest that

Figure 7. Membranous veils and their continuity with the agranular reticulum. Five consecutive sections from a 43-d neurite show that all MTs are surrounded by an electron-lucent zone, 65-nm in diameter. This zone also excludes the membranous veils (*arrowhead*). In *B* and *E*, arms connecting the veils with the AR are seen. Bar, 0.5 μm.

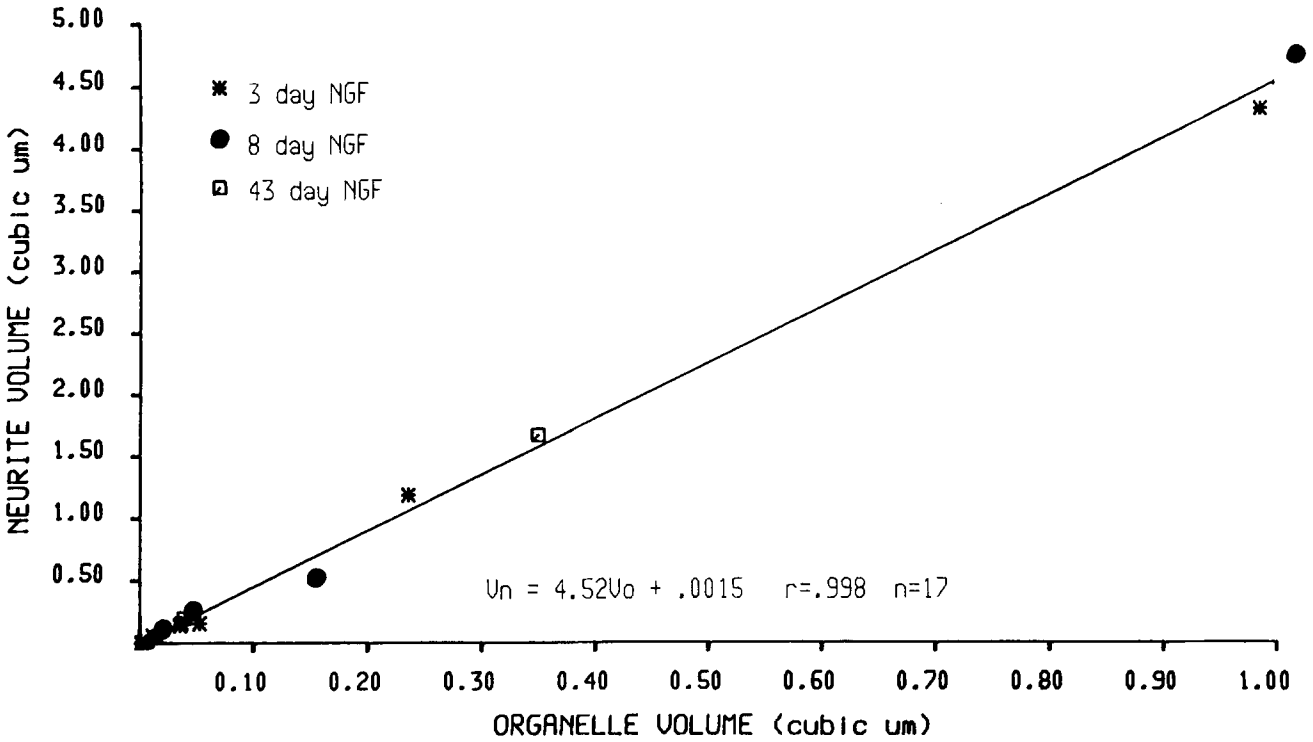

Figure 9. Linear regression of neurite volume to membranous organelle volume. The total volume of all organelles in a varicose neurite region (abscissa) is plotted against the local neurite volume in the same varicose region after correction for MT volume (ordinate). Seventeen neurite regions from 3-, 8-, and 43-d neurites are plotted. Corrected neurite volume is 4.52 times organelle volume ($r = 0.99$). Additional details may be found in Materials and Methods.

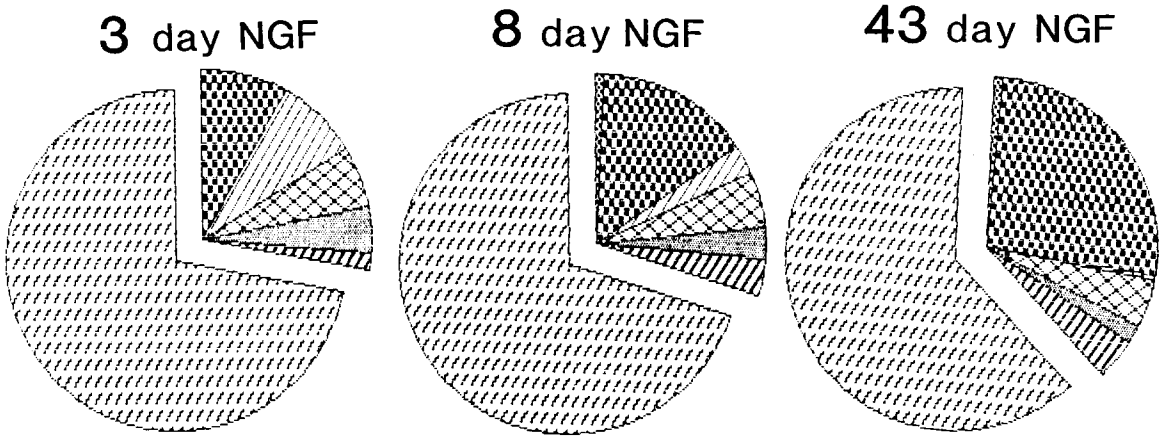

COMPONENT:	% total volume 3 day	8 day	43 day
- UNOCCUPIED VOLUME	72.0	70.6	62.4
- NEUROFILAMENTS	0	1.0	1.0
- MICROTUBULES	8.3	14.8	26.0
- MITOCHONDRIA	7.9	2.8	0.6
- AGRANULAR RETICULUM	5.8	5.3	4.4
- CHROMAFFIN GRANULES	4.4	3.1	1.6
- DENSE BODIES	1.6	3.4	4.0

Figure 10. Changes in relative volume contribution of different organelles during neurite ontogeny. The extruded portion of each pie chart represents the total volume of structures traced in all complete reconstructions. The legend below identifies each portion and the percentage of total volume. MT volume is equivalent to the summed volume of the MT exclusion cylinders.

the diameter of the MT exclusion cylinder is invariant for all ages of PC12 neurites examined. If MAPs are responsible for the exclusion cylinder, then at least the length of the MAPs in the PC12 neurite appear not to change during development.

Only MAP 1 and tau have been subject to detailed analyses in NGF-activated PC12 cells (Greene et al., 1983; Drubin et al., 1985). It has been shown that these MAPs are expressed at low levels in the first few days after NGF activation when a low density of MTs are present in neurites. At the end of 1 wk in NGF, when MTs begin to dominate in neurites, tubulin synthesis has only doubled, while tau and MAP 1 synthesis has risen 20-fold (Feinstein et al., 1984). MAPs have been demonstrated to catalyze MT polymerization from free tubulin (Fellous et al., 1976; Francon et al., 1978; Hesketh, 1984). Free tubulin levels are much higher in young PC12 neurites than in mature neurites (Drubin et al., 1985). Perhaps the massive induction of MAP synthesis is necessary for increased MT density and increased morphological specialization of the neurite.

Microtubule Length

Our data suggest that MTs in PC12 neurites are not continuous. MT terminations are found most frequently in the vicinity of membranous organelles, and these are encountered more frequently in young neurites. We cannot exclude that some portion of these MT breaks actually occur during fixation (Luftig et al., 1977; Chalfie and Thompson, 1979). However, several observations suggest that they may not be artifactual. First, MT endings bear no correlation in position with MT beginnings within any series. That is, if fixation had simply broken an MT we would expect to find a high correlation between MT starts and stops within a series. This argument is pursued in greater detail by Sasaki et al. (1983). Finally, direct microscopic observation during fixation shows no dramatic changes in shape (see the following report), which we might expect if many MTs were being depolymerized.

Several previous calculations of MT length based upon counts in single cross sections have suggested that MTs are continuous (Weiss and Mayr, 1971; Schliwa, 1978; Letourneau, 1982). These results can be explained by the observation that MT density is constant along the length of the axon or neurite. However, serial reconstruction at the electron microscopic level has demonstrated the MTs in axons (Chalfie and Thompson, 1979; Tsukita and Ishikawa, 1982; Bray and Bunge, 1981), dendrites (Sasaki et al., 1983), or the mitotic spindle (McIntosh et al., 1979) are discontinuous structures. Our own data presented in this study, also based upon a total MT reconstruction at the electron microscopic level, supports these previous reconstructions. Moreover, it is hard to imagine that axons which may often reach lengths of many meters, and must stretch by as much as 10–15% during body movement, could possibly have a single set of continuous MTs from soma to termination. The overlapping, discontinuous structure we and others have reported would make more mechanical sense, in that it would provide for a certain forgiving stretch.

Microtubule terminations characterized in serial reconstruction axons (Chalfie and Thompson, 1979) or dendrites (Sasaki et al., 1983) demonstrate some polarity in MT beginnings (tending to be found near membranous organelles) and endings (tending to be found near the plasmalemma). The present reconstructions of PC12 neurites failed to demonstrate this polarity; however, we observe that MT terminations were associated with membranes or organelles.

Intermediate Filaments

Intermediate filaments or neurofilaments were not dominant components of any neurite. IFs were rarely encountered in young neurites, and only in mature neurites did they make a detectable contribution to neurite volume. This is unlike larger axons of the nervous system, where IF volume is a dominant contributor to neurite caliber (Friede and Samorajski, 1970; Berthold, 1978) and has been proposed as a regulator of axon caliber in the peripheral nervous system (Hoffman and Lasek, 1980; Hoffman et al., 1984). Calculated inter-IF distance (26 nm) is much lower than that reported for dorsal root axons in culture (Yamada et al., 1971). It has been noted that IF metabolism in PC12 cells may be aberrant (Lee and Page, 1984) and that some 10-nm filaments in neurites may in fact be vimentin, which is not expressed by normal differentiating neurons. For this reason, PC12 is not a good model for study of the role of NFs in normal neuronal differentiation.

Obligatory Volume

We first described the organelle obligatory volume in a previous paper (Sasaki et al., 1984). We found that each organelle had an associated volume that seemed to occupy space beyond the organelle itself. We also demonstrated that a single varicosity often contained two or three organelles. These organelles all contained within the same varicosity had volumes that were very poorly correlated with each other. Hence it was unlikely that extrinsic factors determined organelle volume. However, the correlation between the total volume of a group of organelles and the volume of the varicosity was always very high (>0.98). Thus, we concluded that the organelles control the neurite volume rather than vice versa.

We find that the PC12 organelles as a group occupy a volume ~4.52 times their own volume, and this figure seems to remain constant throughout development. It is interesting that the major portion of the young neurite's volume is this obligatory volume (see Fig. 10). As the total number of organelles decreases with development, the total contribution made by the obligatory volume also decreases. However, even in the mature neurites, the obligatory volume represents well over 50% of the total neurite. This may at first seem inconsistent with other reports of actin filaments filling the spaces between organelles, however, these data and particularly the data presented in the following paper simply suggest that these actin filaments may not be structural components in the sense they create neurite shape, but rather they may represent a "fill" that occupies the volume controlled by the organelles. The prominent varicosities associated with the organelles seen in Fig. 5 show directly that the organelles and the obligatory volume constant play a direct role in shape control. Additional data and a detailed model will be presented in the following paper.

Agranular Reticulum

The AR is a longitudinally oriented network of interconnecting membranous tubules and cisternae uniformly distributed

in axons (Peters et al., 1976; Berthold, 1978). It has been postulated that this membranous network is continuous in axons (Tsukita and Ishikawa, 1980; Droz et al., 1975) and is continuous with mitochondrial membrane (Franke and Kartenbeck, 1971; Spacek and Lieberman, 1980) and multilamellar bodies (Sotelo and Palay, 1971). Our observations suggest close association of the AR with other membranous organelles, but not physical continuity. Nevertheless, the AR network itself is continuous through the neurite. The organization or volume of the AR does not change dramatically during PC12 neurite development. It is probable that the AR assumes no structural specializations during functional specialization of the neurite. Although axonal functions like fast transport were thought to be AR mediated, recent work has shown this is likely not the case (Lavail et al., 1980; Ellisman and Lindsey, 1983).

Chromaffin Granules

Activation of PC12 cells with NGF results in an increase in the production of 300-nm diameter dense granules. These are ultrastructurally (Luckenbill-Edds et al., 1979; Tischler et al., 1983) and biochemically (Greene and Tischler, 1976; 1982) similar to chromaffin granules of the adrenal medulla or adrenergic neuron phenotype (Elfvin, 1967; Unsicker and Chamley, 1977). Chromaffin granules are not seen in cholinergic neural crest cells. During initial phases of NGF activation, chromaffin granules are found distributed throughout the PC12 soma, but after a few days they migrate into and dominate bulbous extensions from the soma (Luckenbill-Edds et al., 1979; Tischler et al., 1983; Trogadis, J. and J. K. Stevens, unpublished results). These processes are distinguished from immature neurites by their lack of any MT. We find the number of chromaffin granules declines rapidly during development, which has not been noted in other studies (Greene and Tischler, 1982). This may be due in part to our choice of low plating densities for differentiation experiments. High cell density stimulates activity of enzymes of catecholaminergic anabolism (Greene and Rein, 1977; Edgar and Thoenen, 1978), which may result in increased chromaffin granule density in densely plated cells.

Mitochondria

The number and distribution of mitochondria in a neurite process is a measure of the level of aerobic metabolic activity in the neurite. Mitochondrial density is high in young neurites only. Young, extending neurites must be metabolically more active than mature, stable ones. Mature PC12 neurites contain far fewer mitochondria than axons of in vivo origin (unpublished results). This could be accounted for by the metabolic demands of synaptic maintenance, from which PC12 neurites in monotypic culture are exempt.

Dense Bodies

Multivesicular bodies, multilamellar bodies, and large dense granules were grouped in the volume analysis as dense bodies. The functions of these organelles are not clear. Large dense granules could be an intermediate catabolic organelle for recycling of membrane constituents (Peters et al., 1976). The multilamellar body has been postulated to be a storage organelle for AR membrane (Sotelo and Palay, 1971), and more recently to be the retrogradely transported remains of mitochondria (Fahim et al., 1985). The multivesicular body contains and transports vesicles collected by endocytosis (Rosenbluth and Wissig, 1964). These activities should be more prevalent in young neurites when shape and membrane distribution change rapidly, yet young neurites contain many fewer dense bodies than mature ones. The dense bodies represent a large portion of the organelles known to be retrogradely transported, so it is possible that the volume of retrogradely transported organelles rises during development.

Summary and Conclusions

These data allow us to draw a number of important conclusions. First there are several clear changes in cellular organization during the development of PC12 neurites. These changes can be characterized by two major transitions. First, MTs, which define the longitudinal axis of the neurite, increase in number leading to a more cylindrical and uniform neurite shape. Second, there are major changes in the relative numbers of other organelle types, which reflect the functional specialization of the neurite. These changes, however, do not in themselves seriously affect shape change of the neurite during development, however the presence of these organelles and their associated obligatory volumes account for well over 50% of the neurite's volume at all stages of development. We find that the MT–MT distances and obligatory volumes associated with the organelles remain constant throughout development. Thus, we can conclude that many of the observed changes seen in developing PC12 neurites are due simply to the production of a greater number of MTs in the cell, and that many of the other important parameters that can be measured that contribute to neurite volume remain constant during development.

We thank J. Trogadis for her help in this project.

This work was supported by a grant to J. K. Stevens and studentship support to J. R. Jacobs from the Canadian Medical Research Council, and The Kroc Foundation.

Received for publication 25 November 1985, and in revised form 18 April 1986.

References

Behnke, O. 1975. Studies on isolated microtubules. Evidence for a clear space component. *Cytobiologie.* 11:366–381.

Berthold, C. H. 1978. Morphology of normal peripheral axons. *In* Physiology and Pathology of Axons. S. G. Waxman, editor. Raven Press, New York. 3–63.

Black, M. M., and Greene, L. A. 1982. Changes in the colchicine susceptibility of microtubules associated with neurite outgrowth: studies with nerve growth factor-responsive PC12 pheochromocytoma cells. *J. Cell Biol.* 95: 379–386.

Bloom, G. S., and R. B. Vallee. 1983. Association of microtubule-associated protein 2 (MAP2) with microtubules and intermediate filaments in cultured brain cells. *J. Cell Biol.* 96:1523–1531.

Bray, D., and M. Bunge. 1981. Serial analysis of microtubules in cultured rat sensory axons. *J. Neurocytol.* 10:589–605.

Bullock, G. R. 1984. The current status of fixation for electron microscopy: a review. *J. Microsc (Oxf.).* 133:1–15.

Burton, P. R., and H. L. Fernandez. 1973. Delineation by lanthanum staining of filamentous elements associated with the surfaces of axonal microtubules. *J. Cell Sci.* 12:567–583.

Chalfie, M., and J. N. Thompson. 1979. Organization of neuronal microtubules in the nematode *Chaenorhabditis elegans. J. Cell Biol.* 82:278–281.

Connolly, J. L., L. A. Greene, R. R. Viscarello, and W. D. Riley. 1979. Rapid sequential changes in surface morphology of PC12 pheochromocytoma cells in response to nerve growth factor. *J. Cell Biol.* 82:820–827.

Dentler, W. L., S. Granett, and J. L. Rosenbaum. 1975. Ultrastructural localisation of the high molecular weight proteins associated with in vitro assembled brain microtubules. *J. Cell Biol.* 65:237–241.

Dichter, M. A., A. S. Tischler, and L. A. Greene. 1977. Nerve growth factor-induced change in electrical excitability and acetylcholine sensitivity of a rat pheochromocytoma cell line. *Nature (Lond.).* 268:501–504.

Droz, B., A. Rambourg, and H. L. Koenig. 1975. The smooth endoplasmic reticulum: structure and role in the renewal of axonal membrane and synaptic vesicles by fast axonal transport. *Brain Res.* 93:1–13.

Drubin, D. G., S. C. Feinstein, E. M. Shooter, and M. W. Kirschner. 1985. Nerve growth factor-induced neurite outgrowth of PC12 cells involves the coordinated induction of microtubule assembly and assembly-promoting factors. *J. Cell Biol.* 101:1799–1807.

Edgar, D. H., and H. Thoenen. 1978. Selective induction in a nerve growth factor-responsive pheochromocytoma cell line (PC12). *Brain Res.* 154:186–190.

Elfvin, L. G. 1967. The development of the secretory granules in the rat adrenal medulla. *J. Ultrastruct. Res.* 17:45–62.

Ellisman, M. H., and Lindsey, J. D. 1983. The axoplasmic reticulum within myelinated axons is not transported rapidly. *J. Neurocytol.* 12:393–411.

Fahim, M. A., R. J. Lasek, S. T. Brady, and A. J. Hodge. 1985. AVEC-DIC and electron microscopic analyses of axonally transported particles in cold-blocked squid giant axons. *J. Neurocytol.* 14:689–704.

Feinstein, S., D. Drubin, R. Sherman-Gold, M. Kirschner, and E. M. Shooter. 1984. Mobilization of cytoskeleton elements during NGF-induced neurite outgrowth in PC12 cells. *Soc. Neurosci. Abstr.* 10:103.

Fellous, A., J. Francon, A. M. Lennon, and J. Nunez. 1976. Initiation of neurotubulin polymerisation and rat brain development. *FEBS (Fed. Eur. Biochem. Soc.) Lett.* 64:400–403.

Francon, J., A. Fellous, A. M. Lennon, and J. Nunez. 1978. Requirement for factors for tubulin assembly during brain development. *Eur. J. Biochem.* 85:43–53.

Franke, W. W., and J. Kartenbeck. 1971. Outer mitochondrial membrane is continuous with endoplasmic reticulum. *Protoplasma.* 73:35–41.

Friede, R. L., and T. Samorajski. 1970. Axon calibre related to neurofilaments and microtubules in sciatic nerve fibres of rats and mice. *Anat. Rec.* 167:379–388.

Goldfischer, S., Y. Kress, B. Coltoff-Schiller, and J. Berman. 1981. Primary fixation in osmium potassium ferrocyanide: the staining of glycogen, glycoproteins, elastin and intercisternal trabeculae. *J. Histochem. Cytochem.* 29:1105–1111.

Greene, L. A., R. K. H. Liem, and M. L. Shelanski. 1983. Regulation of a high molecular weight microtubule-associated protein in PC12 cells by nerve growth factor. *J. Cell Biol.* 96:76–83.

Greene, L. A., and A. S. Tischler. 1982. PC12 pheochromocytoma cultures in neurobiological research. *Adv. Cell. Neurobiol.* 3:373–414.

Greene, L. A., and G. Rein. 1977. Synthesis, storage and release of acetylcholine by a noradrenergic pheochromocytoma cell line. *Nature (Lond.).* 268:349–351.

Greene, L. A., and A. S. Tischler. 1976. Establishment of a noradrenergic clonal line of rat adrenal pheochromocytoma cells which respond to nerve growth factor. *Proc. Natl. Acad. Sci. USA.* 73:2424–2428.

Hardam, A. R., and B. E. S. Gunning. 1978. Structure of cortical microtubule arrays in plant cells. *J. Cell Biol.* 77:14–34.

Hesketh, J. E. 1984. Differences in polypeptide composition and enzyme activity between cold stable and cold labile microtubules and study of microtubule alkaline phosphatase activity. *FEBS (Fed. Eur. Biochem. Soc.) Lett.* 169:313–318.

Hickey, W. F., A. Stieber, R. Hogue-Angeletti, and J. Gonatas. 1983. Nerve growth factor-induced changes in the Golgi apparatus of PC12 rat pheochromocytoma cells as studied by ligand endocytosis, cytochemical, and morphometric methods. *J. Neurocytol.* 12:751–766.

Hoffman, P. N., J. W. Griffin, and D. W. Price. 1984. Control of axonal caliber by neurofilament transport. *J. Cell Biol.* 99:705–714.

Hoffman, P. N. and R. J. Lasek. 1980. Axonal transport of the cytoskeleton during regeneration: constancy vs. change. *Brain Res.* 202:317–334.

Jacobs, J. R. 1985. The ontogeny of structure and organization of PC12 neurites. Ph.D. Thesis. University of Toronto. 79–104.

Langford, G. M. 1983. Length and appearance of projections on neuronal microtubules in vitro after negative staining: evidence against a cross-linking function for MAPs. *J. Ultrastruct. Res.* 85:1–10.

Lasek, R. J. 1982. Translocation of the neuronal cytoskeleton and axonal locomotion. *Philos. Trans. R. Soc. Lond. B Biol. Sci.* 299:313–327.

Lasek, R. J., and P. N. Hoffman. 1976. The neuronal cytoskeleton, axonal transport and axonal growth. *Cold Spring Harbor Conf. Cell Proliferation.* 3 (Book A):1021–1049.

Lavail, J. H., S. Rapisardi, and I. K. Sugino. 1980. Evidence against the smooth endoplasmic reticulum as a continuous channel for the retrograde axonal transport of HRP. *Brain Res.* 191:3–20.

Lee, V. M., and C. Page. 1984. The dynamics of nerve growth factor-induced neurofilament and vimentin filament expression and organization in PC12 cells. *J. Neurosci.* 4:1705–1714.

Letourneau, P. C. 1982. Analysis of microtubule number and length in cytoskeletons of cultured chick sensory neurons. *J. Neurosci.* 2:806–814.

Luckenbill-Edds, L., C. van Horn, and L. A. Greene. 1979. Fine structure of initial outgrowth of processes induced in a pheochromocytoma cell line (PC12) by nerve growth factor (NGF). *J. Neurocytol.* 8:493–511.

Luftig, R. B., P. N. McMillan, J. A. Weatherbee, and R. R. Weihing. 1977. Increased visualisation of microtubules by an improved fixation procedure. *J. Histochem. Cytochem.* 25:175–187.

Matus, A., G. Huber, and R. Bernhardt. 1983. Neuronal microdifferentiation. *Cold Spring Harbor Symp. Quant. Biol.* 48:77–782.

McIntosh, J. R., K. L. McDonald, M. K. Edwards, and B. M. Ross. 1979. Three dimensional structure of the central mitotic spindle of diatoma vulgare. *J. Cell Biol.* 83:428–442.

Peters, A., S. L. Palay, and H. L. Webster. 1976. The fine structure of the nervous system: the neurons and supporting cells. W. B. Saunders Co., Philadelphia, PA.

Porter, K. R. 1966. Cytoplasmic microtubules and their function. *In* Principles of Biomolecular Organisation. G. E. W. Wolstenholme and M. O'Connor, editors. Churchill, London, pp308–345.

Rosenbluth, J., and S. L. Wissig. 1964. The distribution of exogenous ferritin in toad spinal ganglia and the mechanism of its uptake by neurons. *J. Cell Biol.* 23:307–325.

Sasaki, S., J. R. Jacobs, and J. K. Stevens. 1984. Intracellular control of axial shape in non-uniform neurites: a serial electron microscopic analysis of organelles and microtubules in A1 and AII retinal amacrine neurites. *J. Cell Biol.* 98:1279–1290.

Sasaki, S., J. K. Stevens, and N. Bodick. 1983. Serial reconstruction of microtubular arrays within dendrites of the cat retinal ganglion cell: the cytoskeleton of a vertebrate dendrite. *Brain Res.* 259:193–206.

Schliwa, M. 1978. Microtubular apparatus of melanophores. Three-dimensional organization. *J. Cell Biol.* 76:605–614.

Smith, D. S., U. Jarlfors, and M. L. Cage. 1977. Structural cross bridges between microtubules and mitochondria in central axons of an insect (*Periplaneta americana*). *J. Cell Sci.* 27:235–272.

Sokal, R. R., and F. J. Rohlf. 1969. Biometry. Freeman, Cooper & Co., San Francisco. p374.

Sotelo, C., and S. L. Palay. 1971. Altered axons and axon terminals in the lateral vestibular nucleus of the rat: possible example of axonal remodelling. *Lab. Invest.* 25:653–671.

Spacek, J., and A. R. Lieberman. 1980. Relationships between mitochondrial outer membranes and agranular reticulum in nervous tissue: ultrastructural observations and a new interpretation. *J. Cell Sci.* 46:129–147.

Stebbings, H., and C. E. Bennett. 1975. The sleeve element of microtubules. *In* Microtubules and Microtubule Inhibitors. M. Borgens and M. deBrabander, editors. Elsevier, Amsterdam. 35–45.

Stearns, M. E. 1981. Role of the microtrabecular lattice in axonal transport. *Vision Res.* 21:71–81.

Stevens, J. K., T. L. Davis, N. Friedman, and P. Sterling. 1980. A systematic approach to reconstructing microcircuitry by electron microscopy of serial sections. *Brain Res. Rev.* 2:265–293.

Stevens, J. K., and J. T. Trogadis. 1984. Computer-assisted reconstruction from serial electron micrographs: a tool for the systematic study of neuronal form and function. *Adv. Cell. Neurobiol.* 5:341–369.

Tennyson, V. M. 1970. The fine structure of the axon and growth cone of the dorsal root neuroblast of the rabbit embryo. *J. Cell Biol.* 44:62–79.

Tischler, A. S., L. A. Greene, P. W. Kwan, and V. W. Slayton. 1983. Ultrastructural effects of nerve growth factor on PC12 pheochromocytoma cells in spinner culture. *Cell & Tiss. Res.* 228:641–648.

Tsukita, S., and H. Ishikawa. 1980. The movement of membranous organelles in axons. Electron microscopic identification of anterogradely and retrogradely transported organelles. *J. Cell Biol.* 84:513–530.

Tsukita S., and H. Ishikawa. 1982. The cytoskeleton of myelinated axons. *In* Biological Functions of Microtubules and Related Structures. H. Sakai, H. Mohri, and G. Borisy, editors. Academic Press, Inc., New York. 343–353.

Unsicker, K., and J. H. Chamley. 1977. Growth characteristics of postnatal rat adrenal medulla in culture. *Cell & Tiss. Res.* 177:247–268.

Weiss, P. A., and R. Mayr. 1971. Neuronal organelles in neuroplasmic (axonal) flow. II. Neurotubules. *Acta Neuropathol.* 5(Suppl.):198–206.

Wiche, G., E. Briones, H. Hirt, K. Krepler, U. Artlieb, and H. Denk. 1983. Differential distribution of microtubule-associated proteins MAP1 and MAP2 in neurons of rat brain and association of MAP1 with microtubules of neuroblastoma cells (N2a). *EMBO (Eur. Mol. Biol. Organ.) J.* 2:1915–1920.

Yamada, K., B. S. Spooner, and N. K. Wessells. 1971. Ultrastructure and function of growth cones and axons of cultured nerve cells. *J. Cell Biol.* 49:614–635.